Chapter 3

AIRSAR Implementation

Electromagnetic wave propagation is a vector phenomenon, *i.e.* all electromagnetic waves can be expressed as complex vectors. Plane electromagnetic waves can be represented by two-dimensional complex vectors. This is also the case for spherical waves when the observation point is sufficiently far removed from the source of the spherical wave. Therefore, if one observes a wave transmitted by a radar antenna when the wave is a large distance from the antenna (in the far-field of the antenna), the radiated electromagnetic wave can be adequately described by a two-dimensional complex vector. If this radiated wave is now scattered by an object, and one observes this wave in the far-field of the scatterer, the scattered wave can again be adequately described by a two-dimensional vector. In this abstract way, one can consider the scatterer as a mathematical operator which takes one two-dimensional complex vector (the wave impinging upon the object) and changes that into another two-dimensional vector (the scattered wave). Typically, it is assumed that both the wave impinging upon the scatterer and the scattered wave are spherical waves, due to the finite size of the scatterer. (While this may not be strictly true in the near-field of the scatterer, it is generally true in the far-field. Here we shall not concern ourselves with the exact definitions of the near- and far-field regions of a scatterer. Suffice it to say that for imaging radars, one almost always operates in the far-field of the scatterer, and the spherical wave approximation is valid.) Mathematically, therefore, one can write the scattering process as

$$\mathbf{E}^s = \frac{e^{ikR_1}}{4\pi R_1} \frac{e^{ikR_2}}{4\pi R_2} [\mathbf{S}] \mathbf{E}^i \qquad (3.1)$$

where $\mathbf{E}^s$ is the two-dimensional complex vector representing the scattered wave, $\mathbf{E}^i$ is the two-dimensional complex vector representing the wave impinging on the scatterer, and $[\mathbf{S}]$ is a 2 x 2 complex matrix representing the scatterer. This matrix is known as the *Jones matrix* in optics, after the physicist R. Clark Jones, who in 1941 invented the 2 x 2 complex matrix representation for use in characterization of optical systems and materials. We shall use the more general term *scattering matrix* in this text. In (3.1) R_1 is the distance between the transmitting antenna and the scatterer, and R_2 is the distance between the scatterer and the observation point. The factors ikR_1 and ikR_2 represent the phases of the waves after propagating a distance R_1 and R_2, respectively. Finally, the factors $1/(4\pi R_1)$ and $1/(4\pi R_2)$ denote the spread of the energy as the spherical waves propagate through space. Note that we have not assumed that the transmitting antenna and the observation point are at the same positions in space.

Equation (3.1) forms the basis for radar polarimetry. It says that in order to retain all the information about the scatterer, one has to measure a 2 x 2 complex scattering matrix. In the case of an imaging radar polarimeter, such as the AIRSAR system, one has to measure this complex 2 x 2 scattering matrix for every pixel in a scene. Before going into the detailed AIRSAR implementation, let us first examine (3.1) in order to find the easiest way to measure $[\mathbf{S}]$.

Mathematically, a vector is written in terms of basis vectors. For example, one can write $\mathbf{E}^s$ as

$$\mathbf{E}^s = \begin{pmatrix} E_x^s \mathbf{e}_x \\ E_y^s \mathbf{e}_y \end{pmatrix} \tag{3.2}$$

where $\mathbf{e}_x$ and $\mathbf{e}_y$ are two basis vectors. There is no real reason for these two basis vectors to be orthogonal. If one therefore writes both $\mathbf{E}^s$ and $\mathbf{E}^i$ in terms of basis vectors, it means that one can rewrite (3.1) as

$$\begin{pmatrix} E_x^s \mathbf{e}_x \\ E_y^s \mathbf{e}_y \end{pmatrix} = \frac{e^{ikR_1}}{4\pi R_1} \frac{e^{ikR_2}}{4\pi R_2} \begin{pmatrix} S_{xx'} & S_{xy'} \\ S_{yx'} & S_{yy'} \end{pmatrix} \begin{pmatrix} E_{x'}^i \mathbf{e}_{x'} \\ E_{y'}^i \mathbf{e}_{y'} \end{pmatrix} \tag{3.3}$$

We use primed and unprimed basis vectors to stress the point that the observation point and the transmitting antenna are not necessarily at the same position in space.

Now it is easy to see how one can measure the complete scattering matrix (at least in principle). First, we transmit a vector with one of the components equal to zero, say $E_{y'}^i = 0$. Then, the scattered wave is given by

$$\left.\begin{pmatrix} E_x^s \mathbf{e}_x \\ E_y^s \mathbf{e}_y \end{pmatrix}\right|_{E_{y'}^i = 0} = \frac{e^{ikR_1}}{4\pi R_1} \frac{e^{ikR_2}}{4\pi R_2} \begin{pmatrix} S_{xx'} E_{x'}^i \mathbf{e}_{x'} \\ S_{yx'} E_{y'}^i \mathbf{e}_{y'} \end{pmatrix} \tag{3.4}$$

Thus, by measuring the two components of the scattered-wave field vector, we have measured the first column of the scattering matrix. Similarly, if we transmit a wave with $E_{x'}^i = 0$ it is easy to show that by measuring the two components of the scattered-wave field vector, we would measure the second column of the scattering matrix.

In this chapter, we give an overview of the AIRSAR implementation of measuring the complete scattering matrix. We shall discuss the details of implementing each of the subsystems in Chapter 4.

3-1 Polarimeter Implementation

In practice, the basis vectors mentioned in the previous section represent the polarizations of the radar antennas. Almost always, the polarizations are chosen to be orthogonal. In the AIRSAR system, we have implemented the polarimeter using the linear vertical and horizontal polarizations as our basis. Of course, no antennas are ever perfect; one always transmits or receives a little bit of the orthogonal polarization. This is known as antenna cross-talk and can be removed from the data after processing by using calibration algorithms (van Zyl, 1990).

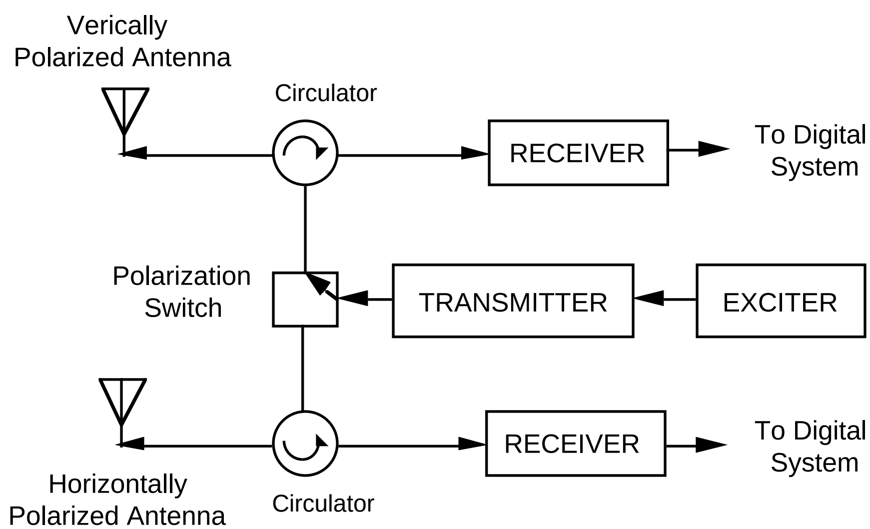

Figure 3.1. *Functional block diagram of one of the three AIRSAR radars.*

Figure 3.1 shows a functional block diagram of any one of the three AIRSAR radars. A single transmitter is used to generate the pulses to be transmitted. A polarization switch is used to switch this signal between the horizontally and vertically polarized transmit antennas, respectively. During the interpulse periods, signals are received through both antennas using separate but identical receivers. In this way, we measure all the elements of the scattering matrix. For example, the first pulse would be transmitted through the horizontally polarized antenna and signals would be received through both the horizontally polarized and vertically polarized antennas. The next pulse would be transmitted through the vertically polarized antenna, and signals would again be received through both horizontally and vertically polarized antennas. Following the first pulse, we measure S_{hh} and S_{vh}, whereas following the second pulse, we measure S_{hv} and S_{vv}. This implementation is shown schematically in Figure 3.2.

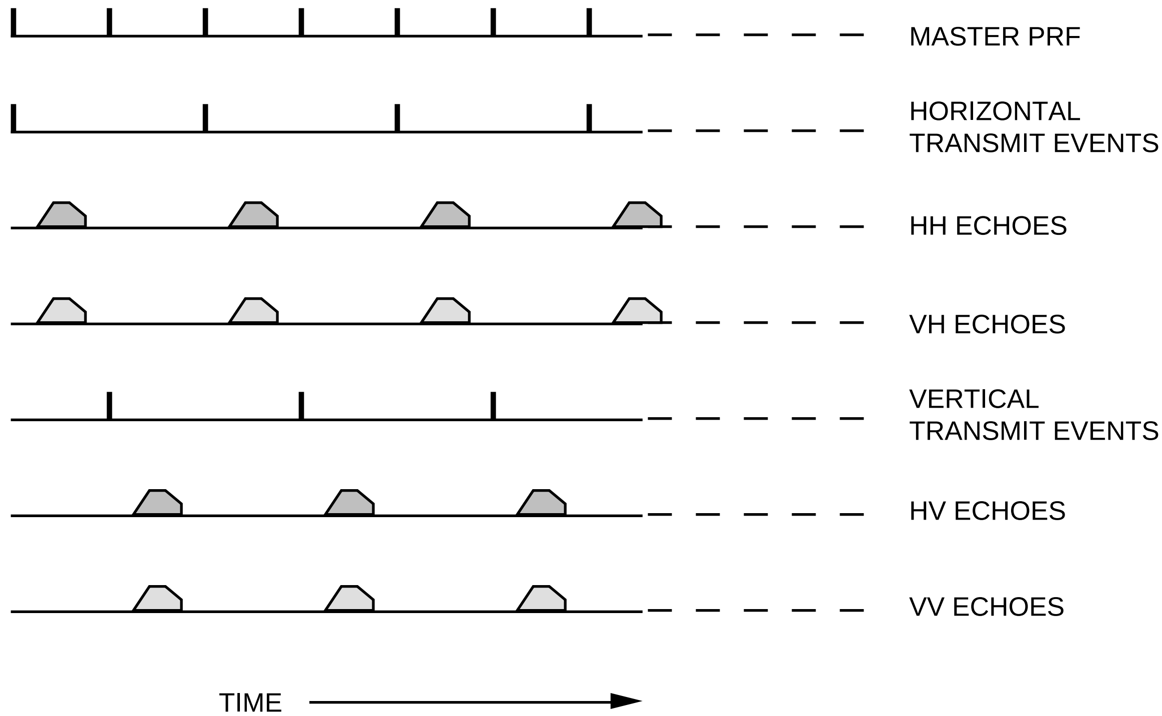

Figure 3.2. *Near simultaneity is achieved from overlapping sets of pulses. Each horizontally polarized transmit pulse and each vertically polarized transmit pulse is offset in time from the other by half the interpulse period, typically 0.5-1 ms. In the data processor, a synthetic aperture is formed by coherently integrating many pulses; however, pulses corresponding to each different polarization combination are isolated and integrated independently from the other pulses. The total coherent integration required to achieve 3 m resolution consists of approximately 1500 pulses over a 2 second period at L-band; therefore, the interspersed sets of pulses correspond to very nearly the same synthesized spatial array.*

With this implementation, each horizontally polarized transmit pulse and each vertically polarized transmit pulse is offset in time from the other by half the interpulse period, typically 0.5-1 ms. In the data processor, a synthetic aperture is formed by coherently integrating many pulses; however, pulses corresponding to each different polarization combination are isolated and integrated independently from the other pulses. The total coherent integration required to achieve 3-m single-look resolution consists of approximately 1500 pulses over a 2 second period at L-band; therefore the interspersed sets of pulses correspond to very nearly the same synthesized spatial array. For example, the DC-8 typically moves at about 400 knots. A 2 second synthetic aperture therefore corresponds to a length of about 400 m. The two sets of synthetic apertures are offset in space by only 10 to 20 cm.

Because the four synthesized spatial arrays are not measured simultaneously, the signals are partially decorrelated. Decorrelation results from the spatial coherence properties of the surface; unless each patch on the surface is viewed from nearly the same direction, the signals will be unrelated. This is the so-called “speckle” effect. In the AIRSAR implementation discussed here, this effect is of little consequence, as the spatial offset between the synthetic apertures is small compared to the system resolution (on the order of 16 m for 16-look data). Consequently, the reduction of cross-correlation intensity in this system for a shift of one interpulse time period out of a coherent integration of 1500 pulses is negligible compared with the total measured intensity, and we can consider to a good approximation that the processed signals arise from synthesized arrays identical in spatial position.

3-2 AIRSAR Hardware Description

The AIRSAR consists of nine racks of hardware, weighing about 1500 kg in total, plus the antennas and the AIRSAR inertial navigational unit. All nine racks of hardware are mounted inside the cabin of a DC-8-72 aircraft, operated by NASA's Ames Research Center in Moffett Field, California. The microstrip patch antennas are mounted fixed to the body on the outside of the aircraft, *i.e.* the antennas are not gimbaled. All antennas are connected to the hardware inside the aircraft cabin via cables. The AIRSAR inertial navigation system is mounted close to the aft antennas in the aft baggage compartment of the DC-8. The radar functions are controlled by a Hewlett-Packard 9000 computer that is mounted in one of the nine racks inside the aircraft cabin.

During data acquisition, the AIRSAR digital system also acquires data from the DC-8 navigational system through the data acquisition and distribution system (DADS) and the AIRSAR inertial navigational unit (INU). In particular, the aircraft ground speed is used by the digital system to set up the pulse repetition frequency (PRF). In the AIRSAR system, the PRF (in Hz) is set to be a constant factor times the aircraft ground speed (in knots). This is done to ensure that successive range lines are recorded at a fixed spacing on the ground, simplifying data processing considerably. (Note that since alternative polarizations are transmitted as shown in Figure 3.2, the actual PRF per channel is half the master PRF.) The control computer also uses the aircraft altitude supplied by the DADS to set the digital recorder delay.

3-2-1 AIRSAR Antenna Subsystem

The AIRSAR antenna subsystem consists of the actual antennas mounted on the side of the DC-8 aircraft, as well as the cables connecting the antennas to the transmitters and receivers, and the switching network that selects the appropriate antennas for the different modes of operation.
The polarimetric antennas are all dual-polarized microstrip patch array antennas. The C-band array consists of 32 patches (two rows of 16 patches each), while the L-band array consists of 16 patches (2 rows of 8 patches each). The P-band array contains only four patches arranged in two sets of two patches each. These antennas are mounted body-fixed to the DC-8 fuselage aft of the left wing. Figure 3.3 shows the aft P-, L-, and C-band antennas mounted on the DC-8.

Figure 3.3. *This photograph shows the aft AIRSAR P-, L- and C-band microstrip patch array antennas. The P-band antenna is mounted on the left, with the C-band antenna mounted above the L-band antenna on the right.*

Other antennas that are considered part of the antenna subsystem include the two C-band antennas used in the TOPSAR mode (see Section 3.3.2. below), and a single L-band antenna mounted in front of the left wing that is used, together with the L-band aft antenna, in the along-track interferometer mode. The TOPSAR antennas can either be single-polarization (vertical) slotted waveguide arrays (manufactured in Italy as part of that country's participation in developing the TOPSAR prototype instrument) or single-polarization (vertical) microstrip patch arrays of the same number of patches as the dual-polarized polarimetric C-band antenna. The front L-band antenna is identical to the one used in the standard polarimetric mode.

3-2-2 AIRSAR RF Subsystem

The AIRSAR radio frequency (RF) subsystem consists of three functionally identical modules (one for each frequency band) and includes a frequency converter, a high power transmitter, and two receivers. In addition, a stable local oscillator (STALO), a digital chirp generator (DCG), and a frequency up-converter comprise shared hardware for all frequency bands. Figure 3.4 shows the functional layout of the AIRSAR radar transmitter system. The STALO provides a master 90 MHz signal from which all other signals in the AIRSAR system are derived. This signal is provided to the DCG, which, in turn, generates a digital chirp pulse and provides that to the L-band transmitter. The chirp is a stepped-frequency FM pulse produced digitally by the DCG. The DCG, which in essence is a numerically controlled oscillator, simulates a linear FM pulse by stepping at a set of pre-selected frequencies within the given pulse width. For the AIRSAR DCG, the frequency-update rate is 5 MHz, *i.e.* the DCG changes to a new frequency every 200 ns. Thus, to generate a 40 MHz chirp with 10 μs duration, 50 frequencies are updated in sequence at equal time intervals within the 10 μs. In the standard AIRSAR polarimetric mode, this reference chirp signal starts at

1258.75 MHz and linearly decreases to 1238.75 MHz in 10 µs. It is also possible to operate the AIRSAR system in a 40 MHz bandwidth mode, in which case the chirp signal would start at 1257.5 MHz and linearly decrease to 1217.5 MHz. In addition, the pulse length may be either 5 µs or 10 µs - see Table 3.1. In the 20 MHz mode, the video frequencies vary from 1.25 MHz to 21.25 MHz, while in the 40 MHz mode, they vary from 2.5 MHz to 42.5 MHz.

Table 3.1 *Possible AIRSAR Polarimetric modes. In both modes, the pulse length may either be 5 µs or 10 µs*

Chirp Bandwidth (MHz)	Chirp Frequencies		
	P-Band (MHz)	L-Band (MHz)	C-Band (MHz)
20	448.75-428.75	1258.75-1238.75	5308.75-5288.75
40	447.5-407.5	1257.5-1217.5	5307.5-5267.5

The L-band chirp signal is up-converted to C-band by mixing it with a 4050 MHz signal derived from the 90 MHz STALO. The up-converted chirp is then provided to the C-band transmitter. At the same time, the L-band chirp is down-converted to P-band by mixing it with an 810 MHz signal derived from the 90 MHz STALO signal and then provided to the P-band transmitter. Transmit polarization diversity in the AIRSAR system is achieved by toggling the polarization switch (see Figure 3.4) in the front ends of the high-power amplifiers. As pointed out before, this means that the transmit event of one polarization is delayed by half of one interpulse period (IPP) to that of the other polarization. Thus, the HH and HV polarizations are not collected simultaneously with the VH and VV polarizations. The effects caused by this difference in transmit timing are compensated for during data processing in such a way that all four polarizations are registered. Travelling-wave tube amlifiers are used at L-band and C-band for the high-power amplifiers, while at P-band a Class C solid-state amplifier, capable of delivering 2 kW peak power, is used. At L-band, the amplifiers can deliver 4 kW peak, and at C-band 1 kW peak power.

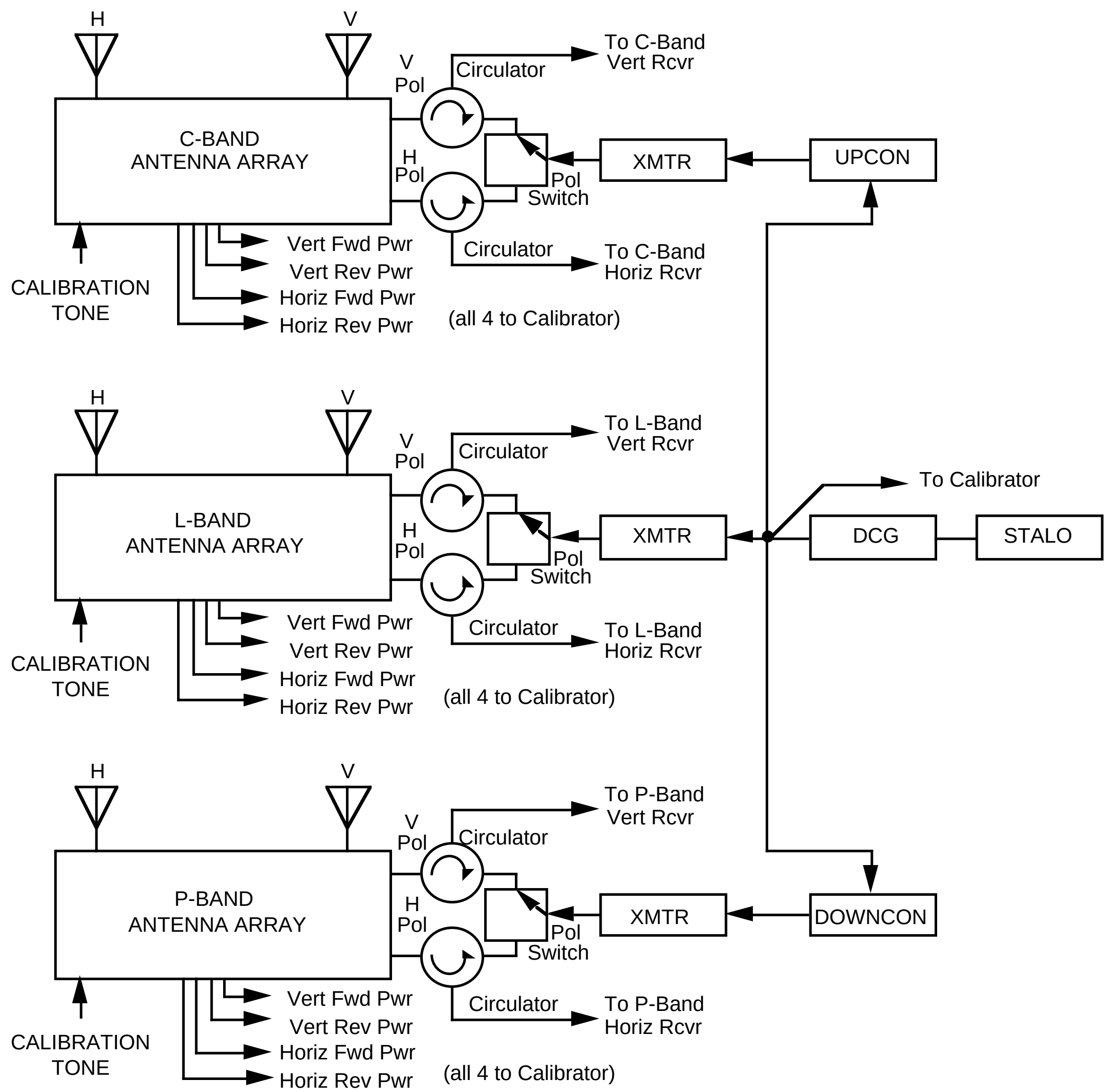

Figure 3.4. *Functional block diagram of the AIRSAR radar transmitter hardware.*

After the chirp waveforms are transmitted, there is obviously some delay before energy is returned to the AIRSAR from the target. This delay is the amount of time required for the transmitted signal to reach the target and then return to the aircraft, and is a function of the aircraft altitude (typically 8000 m above ground level). Upon reception, the returned energy is routed to the receivers by the circulators. The received signals are first heterodyned from the radar frequencies to video frequencies. (In the AIRSAR system, we do not use in-phase and quadrature phase channels when sampling the received signals. Instead, our video signals are offset by one-quarter of the sampling frequency. For example, in the 20 MHz case, the video signals coming out of the receivers are centered at 11.25 MHz. During the data processing, the phases of the received signals are reconstructed using the fact that the transmitted chirp is an analytic signal.) The video output of each receiver is routed to the digital system's analog to digital converter (ADC) for the particular receiver, and the sampled digital data are buffered in that channel's digital buffer. While the use of three stages (two in P-band) of gain control in the receiver greatly increases the overall dynamic range of the receiver, it also imposes a heavy responsibility on the operator to set the gain correctly in order to minimize signal distortion created by saturation in any stage of the receiver chain as well as the ADC small-signal sampling distortion.

3-2-3 AIRSAR Digital Subsystem

Figure 3.5 shows a simplified block diagram of the AIRSAR digital subsystem. The front-end of the digital subsystem consists of six analog to digital converter (ADC) units, one for each receiver channel, (two channels for each frequency). The ADCs digitize the video signals at a pre-selected rate (45 MHz for 20 MHz mode or 90 MHz for 40 MHz mode), at 8 bits per sample. Since all the ADCs are clocked with the same clock signal, the data in the six receiver channels are automatically co-registered. The digitized data samples are stored in high-speed buffers before being multiplexed into a single data stream. However, since the high-speed buffers are limited to 16 kBytes per channel, only a slected portion of the return signal can be stored. A data record window signal selects the appropriate section of the digitized video signals to be stored in the high-speed buffers. The six channels of buffered digital data are transferred to the digital system formatter, where the buffered radar data and engineering telemetry data that are constantly collected by the digital system annotator are combined and formatted into the defined radar range-line data format for the AIRSAR. This formatted data are then transferred to the high-density digital recorder (HDDR) for storage, and at the same time these formatted data are available to an on-board flight correlator which has the ability to provide near real-time image generation. These images provide a means of verifying radar data integrity and radar system health. Before the 1993 flight season, the AIRSAR system used Fairchild Model M85 HDDRs capable of storing data at a rate of 10 MBytes per second. These were replaced by Sony Model DIR-1000 HDDRs for the 1993 flight season and beyond. The Sony HDDRs are capable of storing data at a rate of 32 MBytes per second.

3-2-4 AIRSAR Calibration Network

The calibration network is the key component in the AIRSAR design to allow system testing and monitoring. It consists of a frequency converter with associated filters and amplifiers and a switching network. By means of a five-port directional coupler between the polarization switch and the antenna switches, the calibration network performs two major functions: 1) injection of signals into the receiver chain and 2) measurement of power at various locations in the system.

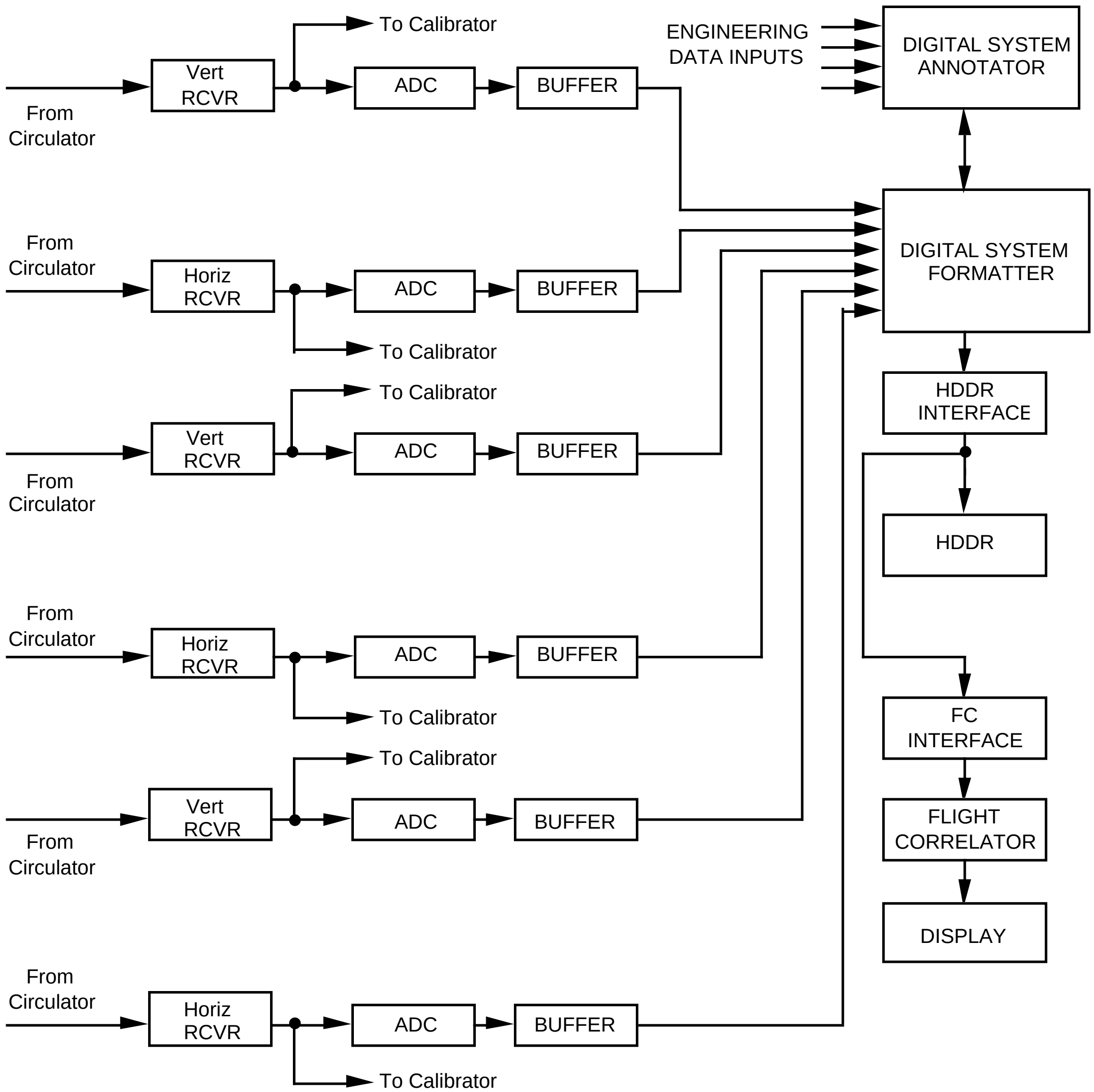

Figure 3.5. *Block diagram of the AIRSAR receivers and digital subsystem.*

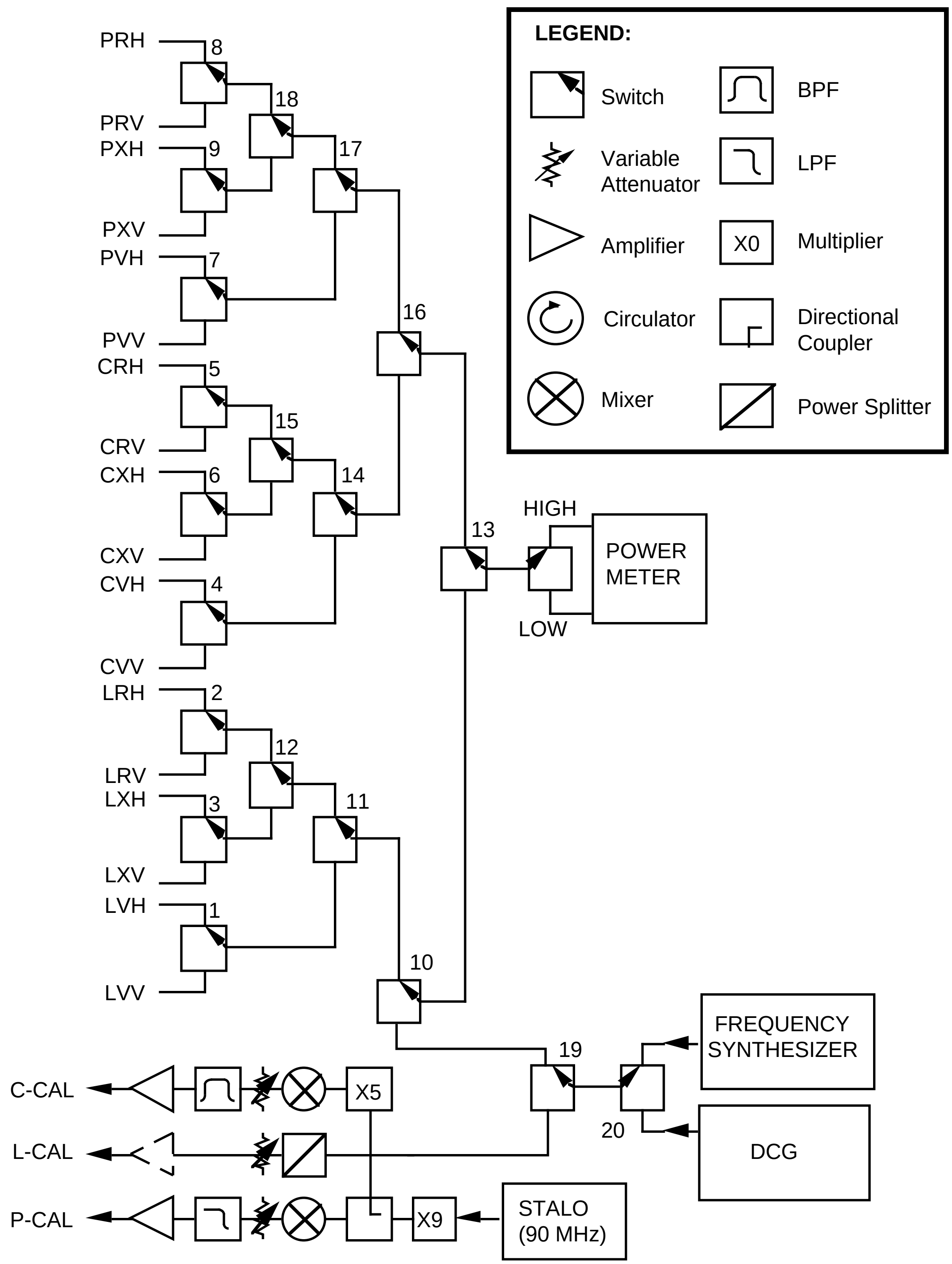

Figure 3.6. *Schematic of the calibration network. The signals are labeled with frequency, followed by R for reflected power, X for transmitted power, and v for video power, followed by the polarization. For example, PRH means the reflected P-band power in the horizontally polarized channel.*

The schematic of the calibration network is shown in Figure 3.6. The switching network consists of a total of 21 electromechanical RF switches (some of them transfer switches). These switches direct one of the 18 inputs to a power meter with selectable thermistor heads to accommodate both high- and low-power measurements. The 18 measurements include the RF transmitted power, the RF reflected power and the down-converted video power for each polarization channel (H and V) at each of the three frequency bands (P, L, and C). Once a desired measurement path is established, the remaining paths are properly terminated. The other function of the switching network is to route an L-band signal, either from a synthesizer or from the up-converted chirp-generator signal, for future up-conversion (C-band) or down-conversion (P-band) and gain control, before injecting it into the receiver chain via the five-port directional coupler. During operational data acquisition, a single-frequency tone, called the calibration tone (caltone) is injected into the recievers using this approach. During data processing, this calibration tone is analyzed and used to measure short-term changes in the receiver gains and phase differences. These measured short-term gain and phase difference changes are then removed in the processor during data calibration.

Table 3.2. *Summary of AIRSAR flight hardware characteristics. The parameters in ( ) apply to 40 MHz configuration.*

Parameter	P-Band	L-Band	C-Band
Chirp bandwidth	20 or 40 MHz	20 or 40 MHz	20 or 40 MHz
Chirp RF frequency	448.75--428.75 MHz (447.50--407.50 MHz)	1258.75--1238.75 MHz (1257.50--1217.50 MHz)	5308.75--5288.75 MHz (5307.50--5267.50 MHz)
Calibration tone	428.5546875 MHz (406.40625 MHz)	1238.5546875 MHz (1216.40625 MHz)	5288.5546875 MHz (5266.40625 MHz)
Video frequency	$450.00 - f_{RF}$ MHz	$1260.00 - f_{RF}$ MHz	$5310.00 - f_{RF}$ MHz
Chirp duration	10 or 5 µs	10 or 5 µs	10 or 5 µs
Peak transmit power	62 dBm	67 dBm	59 dBm
Antenna polarization	H/V dual microstrip	H/V dual microstrip	H/V dual microstrip
Antenna gain	14 dBi	18 dBi	24 dBi
Azimuth beamwidth	19^{o}	8^{o}	2.5^{o}
Elevation beamwidth	38^{o}	44^{o}	50^{o}
Antenna dimensions	91.4 cm x 182.9 cm	45.7 cm x 161.3 cm	16.5 cm x 135.9 cm
Receiver gain	58 dB (59 dB)	50 dB (52 dB)	62 dB (63 dB)
Receiver gain control	> 80 dB	> 80 dB	> 80 dB
Receiver instant. dynamic range	> 40 dB	> 40 dB	> 40 dB
Noise temperature	500-3000 K	500-3000 K	500-3000 K
ADC sampling rate	45 MHz (90 MHz)	45 MHz (90 MHz)	45 MHz (90 MHz)
Bits/ sample	8	8	8

3-3 Principal Investigator Modes

The AIRSAR system also serves as a testbed for new radar techniques. Usually this is done as a service for an approved principal investigator funded by some NASA program. These techniques are usually implemented through a relatively minor modification to the AIRSAR hardware. The AIRSAR group is responsible for the implementation of the special mode, and for the data acquisition for that specific principal investigator only. *The Principal Investigator is responsible for all processing and data distribution.* Therefore, if an investigator wants to utilize one of the principal investigator special modes, it is the responsibility of the investigator to contact the specific principal investigator and arrange for data acquisition and subsequent processing. Note, however, that the flight requests for the principal investigator mode flights are treated the same way as any other flight request that uses the AIRSAR system. Data will only be acquired after approval by the various NASA program offices.

The AIRSAR group currently supports two such principal investigator special modes, Dr. Richard Goldstein's along-track interferometer (ATI) mode, and Dr. Howard Zebker's cross-track interferometer (TOPSAR) mode.

3-3-1 Along Track Interferometer Mode

The along-track interferometer mode is used to measure surface movements. This is done by viewing the same scene at two slightly different times using the same viewing geometry. The phase shift between the two signals measured at the different times can be shown to be proportional to the velocity of the scatterers in the radar look direction.

The along-track interferometer is implemented using two antennas mounted along the fuselage of the DC-8, one in front of the other. Up until the 1991 flight season, the forward antennas were separated from the aft antennas by 20 meters for both L-band and C-band. Because of the way the data are processed and interfered, this means an effective interferometer baseline of 10 meters at both frequencies. At the nominal DC-8 speed, this means a time differential of about 50 milliseconds. Unfortunately, the decorrelation time of the ocean surface is on the order of 10 milliseconds at C-band, which means that the C-band results were compromised significantly by the long baseline.

With the addition of the TOPSAR mode, the chance came to place one of the TOPSAR antennas in such a position as to allow a shorter baseline for the C-band along-track interferometer. Since the decorrelation time of the ocean surface is on the order of 10 milliseconds at C-band, a C-band ATI baseline on the order of two meters is desirable. Unfortunately, due to practical and cost considerations in mounting the antennas on the DC-8, the final baseline between the aft AIRSAR antennas and the bottom TOPSAR antenna is only about one meter.

The along-track interferometer mode is implemented by alternately transmitting out of the aft AIRSAR antenna and the forward antenna, while signals are received simultaneously through the front and aft antennas. In this way, we have implemented two along-track interferometer instruments, one with a baseline of one half the physical separation of the forward and aft antennas, and one with a baseline equal to the physical separation of the forward and aft antennas. The two baselines means that two independent measurements of the surface velocity are made simultaneously. In addition, by measuring the difference in the strength of the correlation of the signals for the two baselines, one is able to estimate the surface coherence time. For more information of the along-track interferometer implementation and use, see Goldstein et al. (1987) or Carande (1993).

3-3-2 Cross-Track Interferometer (TOPSAR) Mode

For the 1991 flight season, we implemented a new special mode, the TOPSAR mode, for Dr. Howard Zebker of JPL. To implement this mode, we added two C-band vertically polarized antennas separated by about two meters, one situated above the other on the fuselage of the DC-8. This implementation allows one to measure topography as described by Zebker and Goldstein (1987).

In the TOPSAR mode, we operate the P- and L-band radars in the standard AIRSAR polarimetric modes. At the same time, the C-band system will be operated in the dual-polarized mode, resulting in a double PRF for the C-band radar. C-band signals are transmitted using the bottom TOPSAR antenna, and received through the top and the bottom TOPSAR antennas simultaneously. With this implementation, the swath widths of all three frequency radars will be the same, although the spacing between successive C-band range lines will be half that of the P-band and L-band data. After the appropriate processing, this mode provides topography data, derived from the C-band data, co-registered with the P-band and L-band polarimetric data.

The prototype processor for the integrated TOPSAR mode, which will produce co-registered topography data and P- and L-band polarimetric data is scheduled to be completed during the summer of 1993. Prototype topography data have been produced by Dr. Howard Zebker since 1991. For more information on the TOPSAR instrument implementation and processing, see Zebker et al. (1992).

3-3-3 Summary of AIRSAR Modes

Table 3.3 shows the possible modes in which the AIRSAR system can be operated. Note that all the modes shown above can be operated with pulse lengths of either 5 or 10 μs and chirp bandwidths of either 20 or 40 MHz.

To summarize, the AIRSAR standard mode is the three-frequency polarimetric mode. The chirp bandwidth is 20 MHz and the pulse length is 10 μs. The AIRSAR system utilizes body-fixed microstrip patch array antennas with dual feeds to achieve polarization diversity upon reception. The polarimeter is implemented by transmitting alternatively out of the two orthogonally polarized antennas. During data processing, this spatial offset of the two synthetic apertures is corrected to ensure that the images register exactly. The received signals are heterodyned down to video frequencies and amplified before being sampled and stored on digital tape. Video-offset sampling, rather than in-phase and quadrature phase channels are utilized when sampling the received signals. During data processing the phases of the original received signals are reconstructed using the fact that the transmitted chirp is an analytical signal.

Table 3.3. *Summary of AIRSAR Modes*

Mode Name	Transmit Antenna	Receive Antenna	Polarization Switch Operating

Quad Polarization (P-, L- and C-band)	Aft H followed by Aft V	Aft H and V simultaneously	Yes
ATI (Before 1991)	P: Aft H followed by Aft V L: Aft H or V C: Aft H or V	P: Aft H and V simultaneously L: Forward H or V and Aft H or V simultaneously C: Forward H or V and Aft H or V simultaneously	P: Yes L: No C: No
ATI (1991 on)	P: Aft H followed by Aft V L: Aft V followed by forward V C: Aft V followed by forward V	P: Aft H and V simultaneously L: Forward V and Aft V simultaneously C: Aft V and Bottom TOPSAR simultaneously	P: Yes L: Yes C: Yes
TOPSAR	P: Aft H followed by Aft V L: Aft H followed by Aft V C: Top TOPSAR	P: Aft H and V simultaneously L: Aft H and V simultaneously C: TOPSAR Top and Bottom simultaneously	P: Yes L: Yes C: No

In addition to the standard polarimetric mode, the AIRSAR instrument can also be operated in one of two interferometer modes; the along-track interferometer mode to measure surface velocities, and the cross-track interferometer mode to measure topography.